Journal of Ovonic Research Vol. 14, No. 3, May - June 2018, p. 177 - 184

THE EFFECT OF NON-UNIFORM FRONT CONTACT RESISTANCE ON PERC SOLAR CELL PERFORMANCE

S. TAHIR[a,b*], A. ALI [b], N. AMIN[b], M. I. ARSHAD[b]
[a]*University of New South Wales, Sydney, NSW 2052, Sydney, NSW 2052, Australia*
[b]*Government College University, Faisalabad 38000 Pakistan*

In this report, we present the simulation of 20.43 % efficiency solar cell using Griddler 2.5 Pro. The cell has a passivated emitter and rear cell (PERC) structure. It is a square *p*-type with local Al-BSF and screen-printed metallization. We have made strip contacts 68 µm wide and 1.4 mm pitch for full area Al- metallization on the rear side of the PERC cell. We have optimized the number of front and rear fingers for the PERC structure. The front contact resistance was also optimized to study the power losses, fill factor losses, recombination currents and saturation current densities at open circuit. We have studied the effect of wrap around (0-25 mm) for the front contact resistance on the output of the Silicon PERC solar cell. It was observed that increase in the wrap around extent from 0 mm to 25 mm had affected the fill factor and efficiency of PERC solar solar cell significantly. The wrap around extent for non-uniformity in front contact resistance showed that the fill factor of PERC solar cell was decreased from 77.87 % to a value of 73.45 %. Whereas the efficiency was decreased from 20.41 % to a value of 19.26 %.

(Received February 28, 2018; Accepted May 3, 2018)

Keywords: Griddler 2.5 Pro, Aluminium Back Surface Field (Al-BSF), Passivated emitter and rear cell (PERC)

1. Introduction

P-type silicon solar cells with aluminium back surface field (Al-BSF) are currently the dominant solar cell technology in high-volume manufacturing, and as the PV industry is trying to enhance the conversion efficiency, the Passivated Emitter and Rear Cell (PERC) [1] cell structure is widely expected to take up increasing market share [2]. The PERC cell structure is different from the full area aluminium back surface field (Al-BSF) solar cell by a passivated rear and localised point contact scheme, which for *p*-type cells is obtained with a plasma enhanced chemical vapour deposition (PECVD) or atomic layer deposition (ALD) deposited AlOx film capped with SiNx on the rear side [3] of the cell.The films deposited by atomic layer deposition (ALD) provide an extremely good level of surface passivation [4, 5], spatial uniformity and precise growth control [6], although spatial ALD systems address the low deposition rates of ALD systems [7]. However, due to the intrinsic nature of the ALD process, unintended deposition of AlOx on the front side of the wafer penetrating up to 1 mm has been reported with destructive consequences, when the AlOx deposition comes before the front side SiNx deposition [8].

The Passivated Emitter and Rear Cell (PERC) structure was introduced to increase the silicon wafer solar cell efficiency. It improves upon the conventional solar cell by replacing the full area Al-BSF (back surface field) on rear surface with a stack of passivation layers and localised contacts. PERC silicon solar cells with rear Al local contacts benefit both from a reduction of recombination at the rear side due to the surface passivation, and an improved carrier generation because of the better optical reflection from the rear side.

The design of the rear-side contact pattern is of critical importance for the performance of a PERC cell. The localised BSF regions can be formed as lines or as an array of points. The selection of the width and pitch of these lines is a trade-off between resistive and recombination

*Corresponding author: sofetahir@gmail.com

losses [9]. The literature showed a variety of values for the recombination at the rear surface and within these localised contact regions.

Computer-based modelling or simulation is standard practice to support solar cell development and characterization. Simulations can optimise the processes and parameters much faster than would be possible by experiment alone. In that way, modelling can improve the understanding of basic device physics and helps to increase solar cell efficiencies. Griddler 2.5 PRO is a powerful solar cell finite element solver that can simulate a solar cell. It can design the metallization pattern with different fingers and busbars geometry for the front and rear side of the solar cell. It can simulate solar cell for single print as well as double print method. It includes different recombination like metal induced recombination and passivation recombination for front as well as rear side of solar cell. Its simulation screen can calculate the rear contact resistance and rear recombination current densities as well. It meshes the front and rear side of solar cell into nodes and triangular elements. After receiving the photocurrent by each node, it can calculate the front and rear voltage at each node and terminal nodes on the front and rear side of solar cell. The solution of these voltages dependent on the front and rear sides of cell is consistent with the current flow pattern for a given cell metallization design and geometry. It also allows the user to apply different optimizations for the improvement of silicon solar cell efficiency. It designs the front and rear grid and then simulates the cell to find V_{oc}, J_{sc}, *FF* and *Eff*. It can also calculate different types of losses including power losses, resistive losses, recombination losses and fill factor losses.

In this research work PERC solar cell was made on large area (156 × 156 mm^2) Silicon wafer, with resistivity 2 Ωcm, and a thickness of 180 µm. We consider phosphorous diffused *n*-type type emitter with single Ag screen-printed metallization and *p*-type base as local rear-full area Al-BSF to make it as PERC cell. Using point contact, instead of line contact is a promising structure for high-efficiency PERC cells, so we have applied strip contact pattern with contact width 68 µm and 1.4 mm pitch on the full area of the rear side. The purpose of this work is to evaluate the effect of full-area AlOx wrap around on the front side of the wafer, when deposited on top of the SiNx film, by simulations.

2. Optimizing the front/rear fingers number

The front metal grid of a solar cell introduces shading losses as well as resistive losses. Cells with different number of fingers have different shading fractions. The total shading fraction is contributed by busbar shading and finger shading [10-12].

$$p_s = p_{s,bus} + p_{s,f} \tag{1}$$

Where p_s is the shading fraction of the entire front metal electrode, $p_{s,bus}$ is the shading fraction of the busbars, and $p_{s,f}$ is the shading fraction of the fingers. The shading by the front metal electrode causes a reduction in short- circuit current. For different numbers of fingers, the short-circuit current density changes as

$$J_{sc} = J_{sc.AA}\,(1 - p_s) \tag{2}$$

Where $J_{sc.AA}$ is the short-circuit current density of the cell's active area (i.e., the areas without metal shading).

For commercial screen-printed silicon wafer solar cells, resistive losses due to the front metal electrode are contributed by busbar resistance, finger resistance, emitter resistance, and contact resistance. The total series resistance of a Si wafer solar cell can be written as [11–13].

$$R_{s.cell} = R_{emitter} + R_{front\ contact} + R_{finger} + R_{busbar} + R_{base} + R_{rear\ contact} + R_{rear\ metal} \tag{3}$$

Where $R_{emitter}$, $R_{front\ contact}$, R_{finger}, and R_{busbar} vary with the front electrode design, and R_{base}, $R_{rear\ contact}$, and $R_{rear\ metal}$ do not. The unvarying series resistance components are called $R_{s.fixed}$. Different numbers of fingers will give different shading fractions and, hence, different J_{sc}, as well as different $R_{s.cell.}$ We used the Griddler 2.5 Pro to design front grid pattern of PERC solar cell for different number of fingers, busbars, front finger contact resistances and different illumination conditions as well to find their effect on solar cell efficiency at room temperature (300 K).

The cell parameters used for modelling are shown in Table 1.

Table 1. Parameters used for modelling.

Parameter	Value	Parameter	Value
Cell shape	Square [9]	Rear finger sheet resistance	10 mΩ/sq [14]
Cell length	156 mm [9]	Front $J_{01\ passivated}$	168 fA/cm^2[9]
Cell width	156 mm [9]	Front $J_{02\ passivated}$	3 nA/cm^2 [15]
Cell thickness	180 µm [9]	Front $J_{01\ metal}$	595 fA/cm^2[9]
Wafer type	P [9]	Front $J_{02\ metal}$	3 nA/cm^2[16]
Ingot diameter	21 cm	Rear $J_{01\ passivated}$	13.1 fA/cm^2 [9]
Front fingers	91 [9]	Rear $J_{01\ metal}$	794.2 fA/cm^2 [9]
Width	60 µm [9]	Wafer resistivity	2 Ω-cm [9]
Front busbar	3 [9]	Rear contact geometry	Strips
Width	1.3 mm [9]	Contact pitch	1.4 mm
Rear finger	119 [9]	Bulk lifetime	371 µs [9]
Width	60 µm [9]	Rear finger contact resistance	5 mΩ-cm^2 [9]
Front finger sheet resistance	2.82 mΩ/sq [15]	Contact SRV	1x10^7 cm/s [9]
Front finger contact resistance	2 mΩ-cm^2 [9]	Front Illumination	1-sun
Front layer sheet resistance	80 Ω/sq [9]	Temperature	25 C

In the present research work simulation were done in Griddler 2.5 Pro by using the parameters given in Table 1. The front busbars were made in two-split style with pointed ends as shown in Fig. 1.

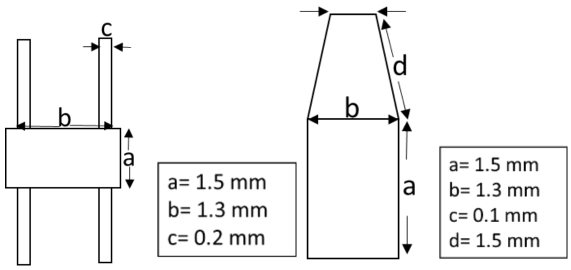

Fig. 1. Front busbars with two-split style and pointed ends.

The single-print method was used for cell metallization. The front finger were tapered from 50 µm over 0.001 cm to reduce the shadowing losses.

We optimize the number of front fingers as well as rear fingers for 70-120 fingers. This optimization showed that 81 fingers on the front side and 70 fingers on the rear side each of width 60 µm results the minimum 4.06 % shading. This decrease in shading results in maximum efficiency of 20.43 %.

Yong e*t* al. also observed a broad maximum in efficiency of silicon solar cell around 75 fingers under STC (25 ^oC, 1000 mW/cm^2, AM 1.5G) conditions [17]. The results obtained by front and rear finger optimization for PERC cell are shown in Table 2.

Table 2. Optimimal front and rear fingers numbers for a PERC solar cell simulated using the parameters listed in Table 1.

V_{oc} (mV)	J_{sc} (mA/cm^2)	FF (%)	Eff (%)	V_{mp} (mV)	I_{mp} (A)	J_{mp} (mA/cm^2)
664	39.51	77.92	20.43	545	9.12	37.49

3. Optimization of front finger contact resistance

To study the optimization of front contact resistance, we used the input parameters given in Table 1. The shading fraction for this metallization pattern was 4.06 %. we optimize the front finger contact resistance for PERC cell from (0.1-100) mΩ-cm^2 by using simulation window of Griddler 2.5 Pro. The results showed that the fill factor as well as the efficiency of PERC cell gradually decreases with the increase of front finger contact resistance from 0.1 mΩ-cm^2 to 100 mΩ-cm^2. The efficiency of the PERC cell varied from 20.51 % to a value of 16.37 % and the results are shown in Fig. 2. The Fill Factor was also decreased from 78.24 % to 62.49 % when the contact resistance increased from 0.1 mΩ-cm^2 to 100 mΩ-cm^2.

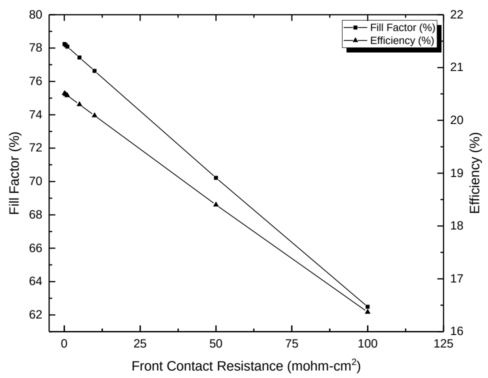

Fig. 2. Effect of Front Contact Resistance on FF and Eff of PERC cell.

Griddler 2.5 Pro simulations are more accurate than any simple power loss formulae. It can calculate the ohmic power dissipation due to lateral current flows in the cell planes by considering the full metallization geometry of the solar cell. The current flow pattern in simple formulae assumes that each node is current source. It also assumes that in H-pattern metallization, current flows in a perpendicular path to the nearest metal finger, then parallel to the finger to the nearest busbar. But these assumptions do not work for metallization other than H-pattern or when the terminal voltage of solar cell is increased beyond the maximum power point.

The power loss chart is shown in Fig. 3. It shows the power output at maximum power point and the contribution of different losses that results in the efficiency of 20.43 % of PERC solar cell. These losses includes the front shading, front resistive losses, rear resistive losses, front recombination losses and rear recombination losses. The front resistive losses show the contribution of contact resistance, finger resistance and semiconductor resistance. Whereas on rear side, mostly contact resistance results in the power losses.

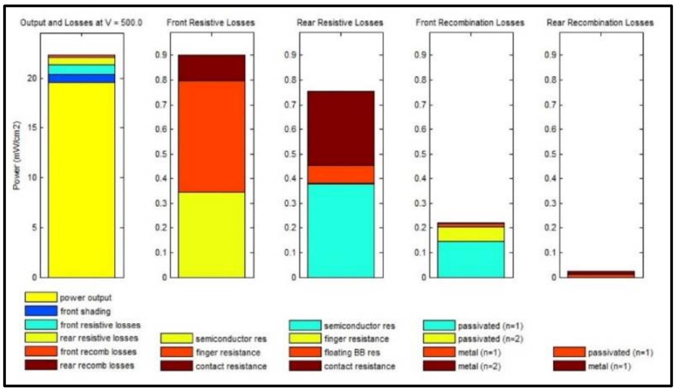

Fig. 3. Power losses bar chart of PERC cell.

It shows the power output at maximum power point and the contribution of different losses that results in the efficiency of 20.43 %. These losses include the front shading, front resistive losses, rear resistive losses, front recombination losses and rear recombination losses as well. The front resistive losses showed approximately 90 % contribution to the power losses of the PERC Silicon solar cell. The front contact resistance, finger resistance and semiconductor resistance contribute 10 %, 45 % and 35 % respectively, to the power losses. Whereas the rear resistive losses contributed almost 75 % to the power losses. Front Recombination losses contribute 20 % to the power loss of PERC Silicon solar cell.

4. Fill factor loss analysis of perc cell

It is extremely important for Silicon solar cell to achieve high fill factors to maximize the power generation capabilities of the cell and module. The fill factor of silicon wafer solar cells is strongly influenced by recombination currents and ohmic resistances as well. We measured the *FF* losses for the PERC Cell simulated by Griddler 2.5 Pro. FF loss analysis of 20.43 % efficient PERC Silicon solar cell is shown in Fig. 4.

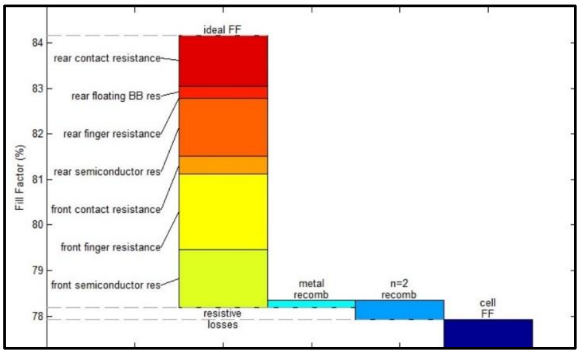

Fig. 4. Fill factor drops water fall diagram.

It was observed that the *FF* dropped from ideal value of 84.3 % to 77.92 % due to front and rear resistive losses. It was dropped from 84.3 % to 78.3 % due to resistive losses. It was further decreased from 78.3 % to 77.92 % (*FF* of our PERC cell) due to recombination currents. It is important to design a solar which minimize the resistive losses as well as recombination currents. The *FF* drops water fall diagram shows that the minimum FF loss has been done by metal recombination currents for the PERC solar cell simulated in this report.

5. The effect of wrap around extent on fill factor and efficiency of PERC solar cell

In this research paper, we have studied the effect of wrap around extent (0- 25 mm) on the fill factor and efficiency of PERC solar cell, by Griddler 2.5 Pro simulations. We have done this by introducing the non-uniformity in front contact resistance at the edges of PERC solar cell for 2 mm, 4 mm, 5 mm, 6 mm, 8 mm, 10 mm, 15 mm, 20 mm and 25 mm. Its effects on the front voltage and rear voltage of PERC solar cell are shown in Fig. 5 and Fig. 6.

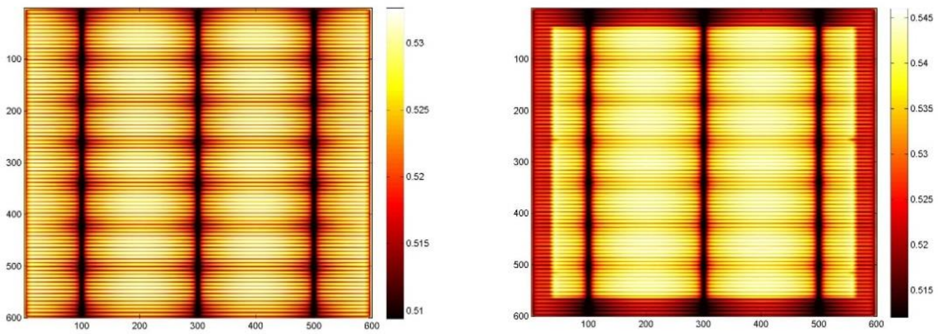

Fig. 5. Front Voltage of PERC cell for 0 mm and 10 mm wrap around extent (left to right).

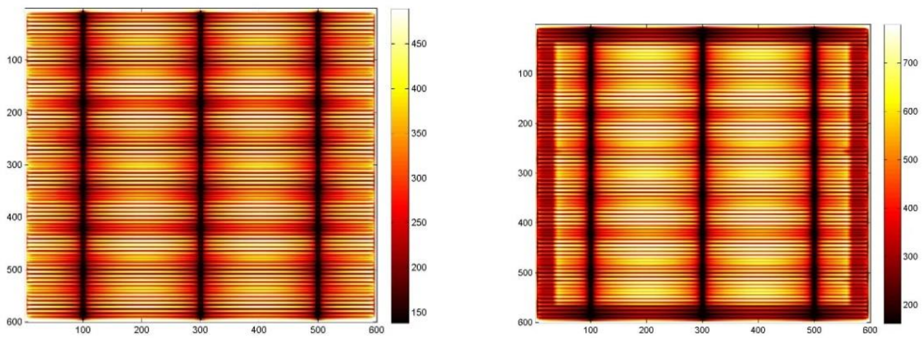

Fig. 6. PL image of PERC cell for 0 mm and 10 mm wrap around extent (left to right).

Both the efficiency and fill factor are reduced with increased wrap-around extent, which represents the increase in series resistance from collecting carriers from the outer affected regions of the cell. This effect is evident in simulated photoluminescence (PL) images of the control (0 mm) and 10 mm wrap around, taken at maximum power point voltage (V_{mpp}) with current extraction, shown in Fig. 6, where areas of higher series resistance have lower luminescence counts. Carriers in areas of higher series resistance are not as effectively collected at V_{mpp} compared to carriers in areas with a lower series resistance, resulting in a lower carrier concentration and consequently lower PL intensity at these areas of high series resistance.

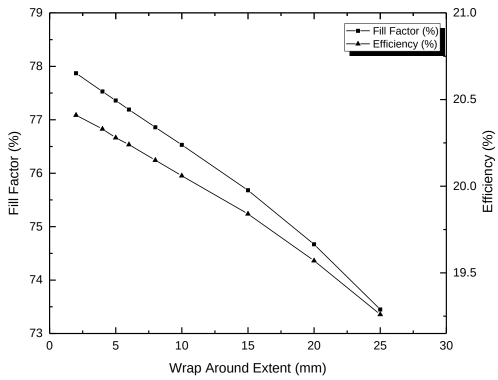

Fig. 7. Effect of Wrap Around Extent on FF and Eff of PERC cell.

The wrap around extent for non-uniformity in front contact resistance showed that the fill factor of PERC solar cell was decreased from 77.87 % to a value of 73.45 %. Whereas the efficiency was decreased from 20.41 % to a value of 19.26 %, as shown in Figure 7.

6. Conclusions

In this work *p*-type silicon wafer with local Al-BSF and single sceen-printed metallization was used to make passivated emitter rear cell (PERC). For this purpose, simulations were made by Griddler 2.5 Pro. We optimized the number of front and rear fingers for improved efficiency and reduced shadowing losses. We found that only 4.06 % shading was present by using 81 tapered fingers and 3 pointed busbars on the front of cell, with maximum efficiency of 20.43 % for PERC cell. We also studied that the increase of front finger contact resistance affects the fill factor and efficiency of PERC cell significantly.

We also found from simulations that the wrap around extent (2- 25 mm) for front contact resistance decreases the *FF* and *Eff* of PERC solar cell significantly. Both the efficiency and fill factor reduce with increased wrap-around extent, which represents the increase in series resistance from collecting carriers from the outer affected regions of the cell. The areas of higher series resistance have lower luminescence counts whereas the areas of lower series resistance have higher luminescence count. Carriers in areas of higher series resistance are not as effectively collected at V_{mpp} compared to carriers in areas with a lower series resistance, resulting in a lower carrier concentration and consequently lower PL intensity at these areas of high series resistance.

Acknowledgements

The authors would like to acknowledge Dr. Bram Hoex, Deputy Head SPREE University of New South Wales Australia, for his sincere guidance during work at UNSW. The authors would like to acknowledge the HEC Pakistan for IRSIP scholarship to do research work at UNSW Australia.

References

[1] G. Dingemans, W. M. M. Kessels, Journal of Vacuum Science & Technology A: Vacuum, Surfaces, and Films **30**(4), 040802 (2012).
[2] A. To, W. M. Li, X. Li, B. Hoex, Energy Procedia **124**, 914 (2017).
[3] Y. Decheng, L. Fang, X. Zhuo, S. Jinchao, L. Gaofei, H. Zhiyan, X. Jingfeng, Journal of Semiconductors **35**(5), 052002 (2014).

[4] T. Grosse, H. P. Sperlich, G. M. Kohler, Proc. 26th Asia Photovolt. Sol. Energy Conf. Exhib., Singapore, 2016.
[5] B. Hoex, M. C. M. Van de Sanden, J. Schmidt, R. Brendel, W. M. M. Kessels, Physica Status Solidi (RRL)-Rapid Research Letters **6**(1), 4 (2012).
[6] J. Wong, Photovoltaic Specialists Conference (PVSC), 2013 IEEE 39th (pp. 0933-0938). IEEE (2013).
[7] D. K. Schroder, Semiconductor material and device characterization. John Wiley & Sons (2006).
[8] J. Qin, W. Zhang, S. Bai, Z. Liu, Applied Surface Science **376**, 52 (2016).
[9] A. Fell, K. R. McIntosh, P. P. Altermatt, G. J. Janssen, R. Stangl, A. Ho-Baillie, K. C. Fong, IEEE Journal of Photovoltaics **5**(4), 1250 (2015).
[10] M. A. Green, Solar cells: operating principles, Technology, and System Applications (1982).
[11] A. Mette, New concepts for front side metallization of industrial silicon solar cells. Verlag Dr. Hut. (2007).
[12] A. R. Burgers, New metallisation patterns and analysis of light trapping for silicon solar cells. Energieonderzoek Centrum Nederland(2005).
[13] H. Hannebauer, M. Sommerfeld, J. Müller, T. Dullweber, R. Brendel, Analysis of the emitter saturation current density of industrial type silver screen-printed front contacts. Proc. 27th EU PVSEC, 1360 (2012).
[14] P. Saint- Cast, S. Werner, J. Greulich, U. Jäger, E. Lohmüller, H. Höffler, R. Preu, Physica Status Solidi (a), **214**(3) (2017).
[15] T. Dullweber, S. Gatz, H. Hannebauer, T. Falcon, R. Hesse, J. Schmidt, R. Brendel, Progress in Photovoltaics: Research and Applications **20**(6), 630 (2012).
[16] W. Deng, D. Chen, Z. Xiong, P. J. Verlinden, J. Dong, F. Ye, Y. Chen, IEEE Journal of Photovoltaics **6**(1), 3 (2016).
[17] Y. S. Khoo, T. M. Walsh, A. G. Aberle, IEEE Journal of Photovoltaics **3**(2), 716 (2013).